Two-dimensional filter bank design for velocity estimation in Forward Scatter Radar configuration

N. Ustalli, F. Di Lello, D. Pastina, C. Bongioanni, S. Rainaldi, P. Lombardo

DIET Department, Sapienza University of Rome
Via Eudossiana, 18 - 00184 Rome, Italy
email: nertjana.ustalli@uniroma1.it

Abstract: *The focus of this paper is on the estimation of the velocity of moving targets with a Forward Scatter Radar system. To this aim a two-dimensional filter bank is proposed with the generic filter impulse response depending on the target electrical size and on the target trajectory that are a priori unknown. In order to limit the computational load required by the bank for practical applications, a two-step processing is proposed: in the first step a rough estimate of the target cross-baseline velocity component is obtained by applying the Radon transform to the spectrogram of the acquired signal while in the second step the bank is exploited to refine the velocity estimation provided by the previous step and also to provide a rough estimation of the target electrical size. The performance of the proposed approach is analyzed against synthetic data under different case studies such as different motion directions, baseline crossing points and different target dimensions. Finally results obtained by applying the proposed processing to FM-based passive FSR experimental data are shown demonstrating the effectiveness of the considered approach.*

1. Introduction

A Forward Scatter Radar configuration can be described as a bistatic configuration where the bistatic angle is close to 180°, [1]. The FSR configuration leads to significant advantages as the enhanced radar cross-section in the forward direction compared to traditional monostatic radar, a possibly long integration time due to little phase and amplitude fluctuation, robustness to the stealth technology and the possibility to operate with transmitters of opportunity such as DVB-T, GSM, DAB, FM etc.,[3],[6]. However the FSR configuration presents some limitations such as the absence of the range resolution and a narrow detection area close to the baseline.
In this paper the issue of velocity estimation of a moving target by exploiting the FSR configuration is addressed. In the past different studies have shown good possibilities to estimate the kinematic parameters in single node FSR configuration (mainly the cross-baseline velocity component) or multistatic/MIMO multi-node FSR configurations (by exploiting the information concerning the time instants at which the target crosses the individual baselines), [2],[4].
In particular in this work, following the line in [2], we refer to a single node configuration and we derive a two-dimensional bank of filters matched to the cross-baseline component of the target velocity and to the size of the target shadow contour. To support practical applications a two-step processing is proposed for the implementation of the bank: *(i)* in the first step a rough estimate of the target cross-baseline velocity component is obtained by estimating the Doppler rate through the Radon transform applied to the spectrogram of the acquired signal *(ii)* and in the second step the bank is exploited to refine the estimate of velocity provided by the previous step and to provide also a rough estimation of the target size. Obviously this greatly reduces the dynamic range of Doppler rate values to be investigated by the bank thus reducing the required computational load. The performance of the considered approach is firstly analyzed against

synthetic data under different case studies and finally its effectiveness and feasibility is demonstrated by using FM-based passive FSR experimental data.
The paper is organized as follow. The forward scatter geometry and the signal model are brefly introduced in section II. The two-dimensional filter bank design algorithm which include the definition of the impulse response and the procedure of the velocity estimation is described in section III. While performance analysis and aspects of filter bank design are discussed in section IV. Experimental set-up and results of aircraft detection and velocity estimation are shown in section V. Conclusion closes the paper.

2. Signal model in Forward Scatter geometry

The main peculiarity of the FSR with respect to the conventional radar systems (i.e monostatic and bistatic configuration) lies in the target scattering nature where the desired signal is due to the shadow of the emitted electromagnetic energy, which occurs in the opposite side of the source from a target whose dimensions are large relative to the incident wavelength, λ,[1]. In this work a target in the far field area of both the transmitter and the receiver is considered. That is, $S = 2d^2/\lambda R < 1$, where R is the distance between the target and the transmitter (receiver) and d is the maximum dimension of the target.
Previous works have shown that the scattering signal in the forward direction is determined by the geometry parameters, the motion parameters of the target and the size of the shadow contour under the assumptions that the target can be thought as a secondary antenna, [1],[2].
The system geometry considered in this analysis is shown in the Figure 1 where the transmitter and the receiver locations are denoted by Tx and Rx, respectively and the transmitter-to-receiver baseline is denoted with L. The origin of the coordinate system corresponds to the location of Rx meanwhile Tx is along the y-axis. $R_T(t) = \sqrt{x(t)^2 + [L - y(t)]^2}$ $\left(R_R(t) = \sqrt{x(t)^2 + y(t)^2} \right)$ is the distance between Tx (Rx) and target and $\theta_T(t) = \tan^{-1}[x(t)/L - y(t)]$ $(\theta_R(t) = \tan^{-1}[x(t)/y(t)])$ is the transmitter (receiver) viewing angle that both vary with time as the target moves.

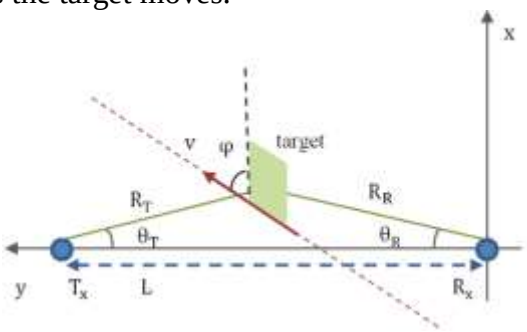

Figure 1 - FSR configuration.

In such FSR configuration, the received signal (in the absence of disturbance) is the sum of the direct signal from the transmitter and the scattered signal in the forward direction due to the presence of the target.
Let the transmitted signal be a continuous wave (CW), at an assigned carrier frequency, f_c with an amplitude a. In agreement with the free space propagation model the complex envelope of the received direct signal taking into account only the path propagation losses is equal to $s_d(t) = \frac{a}{L} e^{j\frac{2\pi}{\lambda}L} = \alpha$.
In this study we assume a rectangular shaped target with horizontal dimension l_h and vertical dimension l_v : the target moves with a constant velocity, v and with direction specified by the angle φ with respect to the normal to the baseline. Hence the target coordinates change with

times, $\begin{cases} x(t) = x_0 + v_x t \\ y(t) = y_0 + v_y t \end{cases}$ where $x_0 = 0$ is assumed, y_0 is the baseline crossing point and (v_x, v_y) are the velocity component v along the x and the y-axis, respectively.
In the literature, it is shown that the target scattered signal due to the target movement has an appropriate Doppler shift with an amplitude modulation specified by the FS pattern, which in turn depends on the shape of the shadow contour and on the motion parameters, [1],[2]. The resulting target signal can be written as $s_t(t) = \beta \varepsilon_t(t) e^{j\varphi_t(t)} = \beta s_{t0}(t)$ where β is a complex factor that takes into account the propagation losses and is proportional to the target dimensions and to the transmitted signal, $\varepsilon_t(t)$ is the FS pattern and $\varphi_t(t)$ is the phase variation. For a rectangular target that follows a linear trajectory the above target parameters are [4],[7]:

$$\begin{aligned} \beta &= j \frac{l_v l_h}{\lambda L} \frac{a}{L} e^{j\frac{2\pi}{\lambda}L} \\ \varepsilon_t(t) &= \frac{L^2}{R_T(t) R_R(t)} \frac{\cos(\theta_T(t) - \varphi) + \cos(\theta_R(t) + \varphi)}{2} \\ &\quad \cdot sinc\left\{\frac{l_h}{\lambda}[\sin(\theta_T(t) - \varphi) + \sin(\theta_R(t) + \varphi)]\right\} \\ \varphi_t(t) &= \frac{2\pi}{\lambda}[R_T(t) + R_R(t) - L] \end{aligned} \tag{1}$$

3. 2D filter bank design

A technique based on a two-dimensional bank of filters is here considered and the procedure for velocity estimation is derived.
Under the assumption of presence of Additive White Gaussian Noise (AWGN), the received signal is $r(t) = s_d(t) + s_t(t) + n(t)$ where $n(t)$ is the noise contribution with variance σ_n^2. The target Doppler signature carrying the kinematic information may be extracted following the processing scheme in [1]. The received signal, $r(t)$ is passed in a square law detector which is followed by a filtering stage to remove the continuous component (DC). The DC removal filter is performed through the cancellation of the mean value from the square signal, $z(t) = |r(t)|^2$ estimated on the entire observation time T. Disregarding the contributions related to $|s_t(t)|^2$ and $|n(t)|^2$we have, [7]:

$$y(t) = z(t) - \frac{1}{T} \approx 2\Re\{\alpha^* \beta s_{t0}(t)\} + 2\Re\{n(t)(\alpha + \gamma\beta s_{t0}(t))^*\} \tag{2}$$

where $\Re\{\cdot\}$ is the real part operator and $(\cdot)^*$ denotes the complex conjugate. The $2\Re\{\alpha^* \beta s_{t0}(t)\}$ is now the desired signal and $2\Re\{n(t)(\alpha + \gamma\beta s_{t0}(t))^*\}$ can be seen as the new component of noise. Therefore resorting to the matched filter theory, [2], the impulse response of the matched filter is:

$$h(t) = \varepsilon_t(t) \sin\left(-\frac{2\pi}{\lambda}[R_T(t) + R_R(t) - L]\right) \tag{3}$$

This implies that $h(t)$ depends on the FS pattern signature and the Doppler signature which in turn depend on the target electrical size and target trajectory that are a priori unknown. This also means that targets with different dimension, different velocity and different baseline crossing angle and crossing point have different signatures.

To address this issue a two-dimensional bank of matched filters is realized and aiming to simplify the analysis the global target signature, $s_{t0}(t)$ is approximated using Taylor series expansion.
More precisely, the phase signature, $\varphi_t(t)$ is approximated by means of a Taylor expansion of the bistatic distance at second-order around the crossing-time instant, t=0 sec:

$$\varphi_t(t) = \frac{\pi}{\lambda} v_x^2 \left[\frac{1}{(L-y_0)} + \frac{1}{y_0}\right] t^2 = -\pi \mu t^2 \tag{4}$$

where, by referring to the system geometry in the Figure 1, y_0 is the distance target-receiver and $L - y_0$ is the distance target-transmitter when the target is on the baseline. In accordance with eq. (4) it is clear that μ is the Doppler rate, $\mu = -\frac{1}{2\pi}\frac{d^2\varphi_t(t)}{dt^2}$ that is function of the cross baseline velocity, v_x and of the baseline crossing point, y_0 for an assigned system geometry (λ and L known).
On the other hand, the pattern signature is approximated by means of a Taylor expansion at first-order around the crossing-time instant:

$$\varepsilon_t(t) = \frac{L^2}{y_0(L-y_0)} \frac{v_x}{v} sinc\left[\frac{l_h}{v}\frac{v_x^2}{\lambda}\left(\frac{1}{L-y_0} + \frac{1}{y_0}\right) t\right] \tag{5}$$

Hence substituting eq. (4) and eq. (5) into eq. (3) and disregarding scale factors, the impulse response of the matched filter become:

$$h(t) = sinc(\mu \eta t)\sin(\pi \mu t^2) \tag{6}$$

where $\eta = \frac{l_h}{v}$. We note that the Doppler rate μ and the parameter η define the width of the main lobe of the pattern signature, $\theta = \mu\eta$, that specifies the main contribution of the energy of the received target signal.
Since both the Doppler rate μ and the width of the main lobe θ are unknown a two-dimensional filter bank is designed:

$$h_{\mu,\theta}(t) = sinc(\theta t)\, sin(\pi \mu t^2) \tag{7}$$

Collecting the samples of the signal in a Nx1 column vector the output of each filter is evaluated as follows:

$$\boldsymbol{\chi}_{\mu,\theta}[i] = \frac{1}{\sqrt{\sum_m \boldsymbol{h}_{\mu,\boldsymbol{\theta}}^{\boldsymbol{2}}[m]}} \sum_{k=0}^{N-1} \boldsymbol{h}_{\mu,\boldsymbol{\theta}}[i-k]\boldsymbol{y}[k] \tag{8}$$

where $\boldsymbol{\chi}_{\mu,\theta}[i]$ is the i-th sample of the output of the filter with impulse response $\mathbf{h}_{\mu,\theta}$ for $i = 1 \ldots 2N-1$. The notation $\mathbf{h}_{\mu,\theta}$ ($\boldsymbol{\chi}_{\mu,\theta}$) is used to indicate that the impulse response and the output vectors of each filter are function of both, the Doppler rate and the width of the main lobe.
Let us define:

$$\Delta(\mu,\theta) = \max_i \boldsymbol{\chi}_{\mu,\theta} \tag{9}$$

for $i = 1 \ldots 2N-1$; the function $\Delta(\mu,\theta)$ has its maximum value for $(\tilde{\mu},\tilde{\theta})$ indicating the estimated Doppler rate and main lobe width which correspond to the matched filter providing the highest output. Thus, in agreement with eq. (4), we can estimate the speed of the target for known baseline crossing point and baseline crossing angle, $\tilde{v}$. Also the horizontal dimension of

the shadow aperture of the target approximated as a rectangular target, $\tilde{l}_h$ can then be estimated giving a rough idea of the target dimensions.
To support practical applications a two-step processing is here proposed for the implementation of the bank (Figure 2): in the first step the Short Time Fourier Transform (STFT) is performed to the signal at the output of the DC removal filter. The STFT has shown good capabilities at extracting kinematic information for a target in the far field area through an FSR configuration, [6].

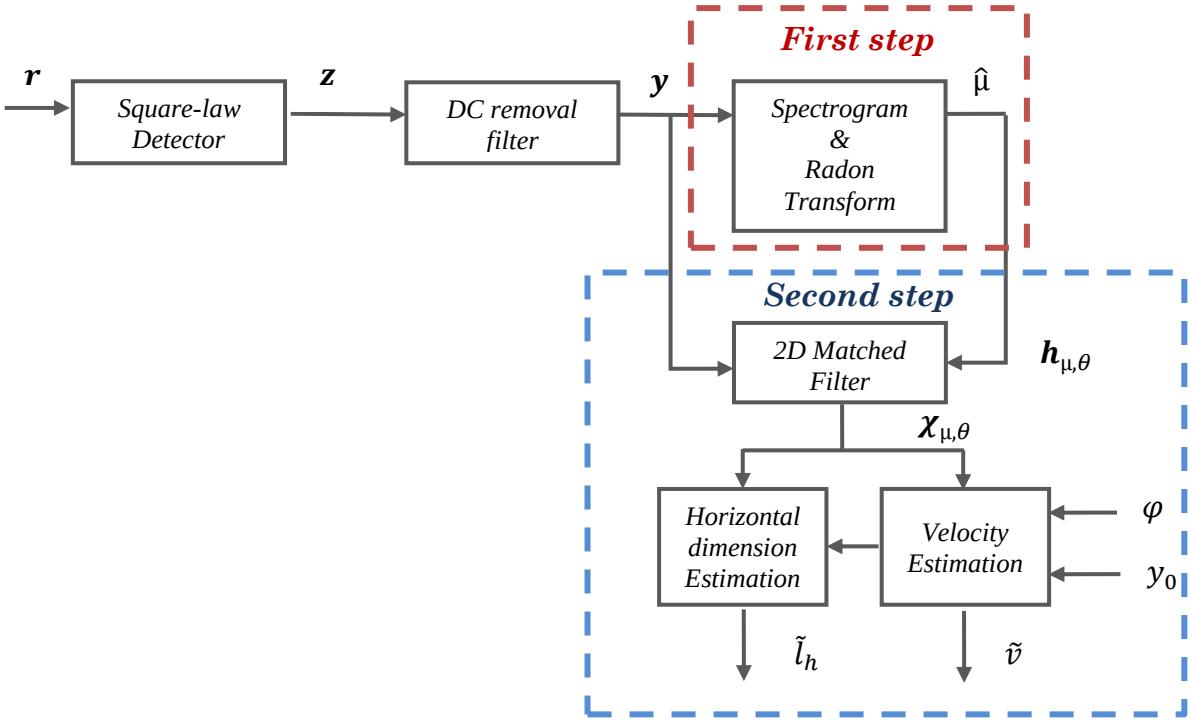

Figure 2 - 2D Matched Filter based algorithm for velocity estimation

The STFT is given by,[8]:

$$S_y[n,k] = S_y\left[n, {}^{2\pi k}/_{M}\right] = \sum_{m=0}^{L-1} y[n+m]\, w[m] e^{-j({}^{2\pi}/_{M})km} \qquad (10)$$

where $w[m]$ is the analysis window of length L (i.e. $w[m] = 0$ outside the interval $0 \leq m \leq L-1$) and $M \geq L$ .With the STFT a linear phase term is compensated which should be sufficient for short enough time window. Since the STFT is a complex-value in general, we used the so called spectrogram that is the squared magnitude of the short-time Fourier transform, $\left|S_y[n,k]\right|^2$. The Radon transform, [9], is then applied to $\left|S_y[n,k]\right|^2$ and a preliminary rough estimate of the target Doppler rate $\hat{\mu}$ is obtained as from the absolute maximum observed on the Radon plane. This greatly reduces the dynamic range of Doppler rate values to be investigated by the bank in the second step thus limiting the required computational load.
As an example Figure 3 reports a double-sided chirp received signal after DC removal filter in the absence of noise for a rectangular target in the far field area that crosses the baseline perpendicularly and in the middle. In addition in Figure 4 the related spectrogram (normalized with respect its maximum value), Figure 4a, and the Radon transform, Figure 4b, are shown obtained for a long observation time, $T = 6.5$ sec and a Hamming window for the estimation of the STFT equal to 0.3 sec. The two red straight lines superimposed to the spectrogram in Figure 4a represent the target Doppler frequency as a function of time as reconstructed by means of the rough estimate of the chirp rate achieved from the Radon transform: it can be

noted that a good initial Doppler rate estimation is provided. Such preliminary estimation is further refined by the two-dimensional bank.

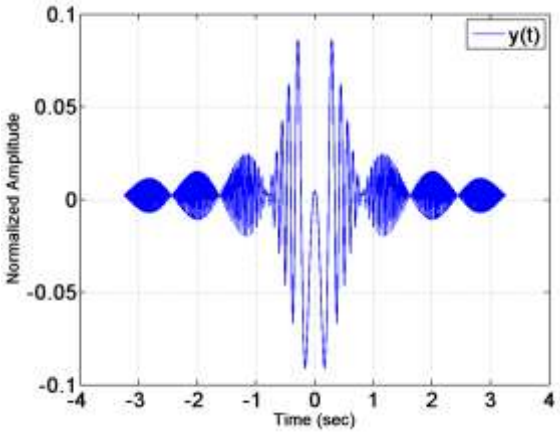

Figure 3 - Received signal after DC removal filter in the absence of noise for a target crossing the baseline perpendicularly in the middle.

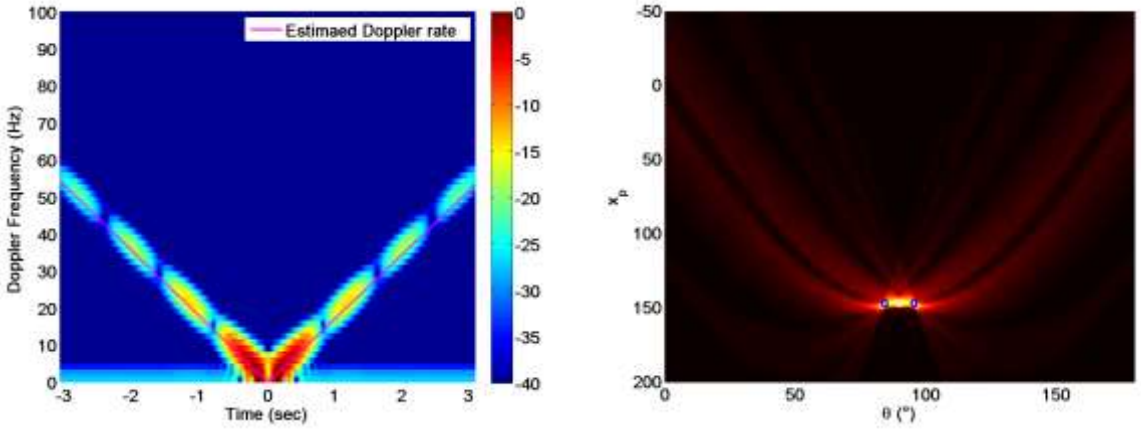

(a) (b)

Figure 4 - (a) Spectrogram and (b) Radon transform for a target crossing the baseline perpendicularly in the middle.

4. Performance analysis

In this section, the performance of the velocity estimation through the 2D filter bank is assessed and discussed for different target trajectories and dimensions.

We consider a carrier frequency $f_c = 4.612GHz$ ($\lambda = 6.5\ cm$), a baseline length equal to L = 4500 m, a long observation time and a rectangular target (with size >> λ) in the far filed area that follows a linear trajectory at constant speed ($v = 36\ m/s$). Four different case studies are investigated, defined by the baseline crossing point, the baseline crossing angle and the target dimensions as shown in the Table I.

According to the processing chain in Figure 2, after an initial estimation of the Doppler rate through the spectrogram and the Radon transform, the impulse response in eq. (7) is constructed considering *(i)* different values of the Doppler rate in the range $\mu = [-15: 0.05: 15] + \hat{\mu}$, where $\hat{\mu}$ is the estimated Doppler rate from Radon transform, and *(ii)* different values of the main lobe width in the range $\theta = [0.1: 0.1: 8]\theta_{theo}$, where θ_{theo} is the theoretical main lobe width of the target.

As a rule of thumb, the Doppler rate step has been chosen taking π/4 as the maximum tolerable phase error; for the main lobe width, the step size has been set in order to guarantee that the energy loss is not more than 10% .

Table I Case studies parameters

	Target dimensions	*Baseline crossing point*	*Baseline crossing angle*
Case A	$l_h = 2.5\ m, l_v = 1.5\ m$	$y_0 = L/2$	$\varphi = 0°$
Case B	$l_h = 2.5\ m, l_v = 1.5\ m$	$y_0 = L/2$	$\varphi = 45°$
Case C	$l_h = 2.5\ m, l_v = 1.5\ m$	$y_0 = L/4$	$\varphi = 0°$
Case D	$l_h = 1.5\ m, l_v = 0.5\ m$	$y_0 = L/2$	$\varphi = 0°$

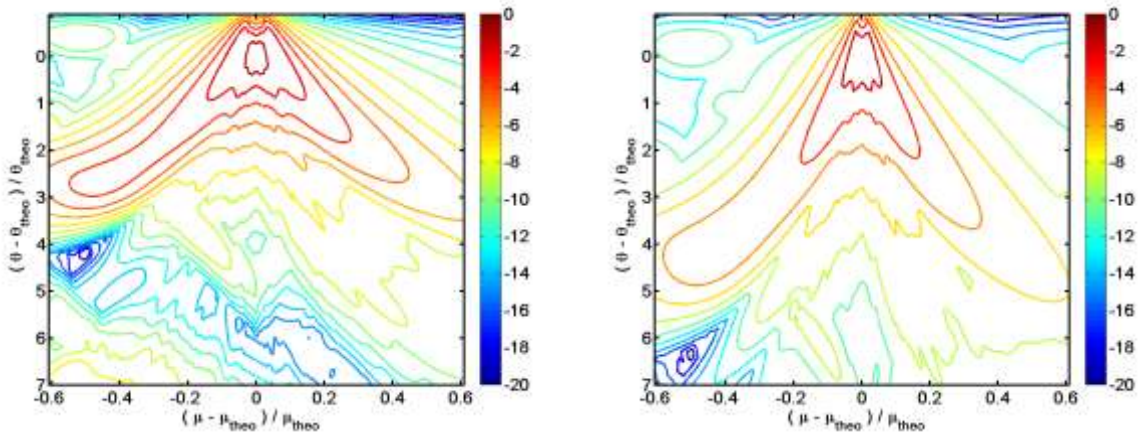

(a) (b)

Figure 5 - Contour plot of $\Delta(\mu, \theta)$ as function of the normalized Doppler rate error and of the normalized main lobe width error (a) for a perpendicular and midpoint crossing baseline, Case A and (b) for a midpoint and non-perpendicular crossing baseline, Case B

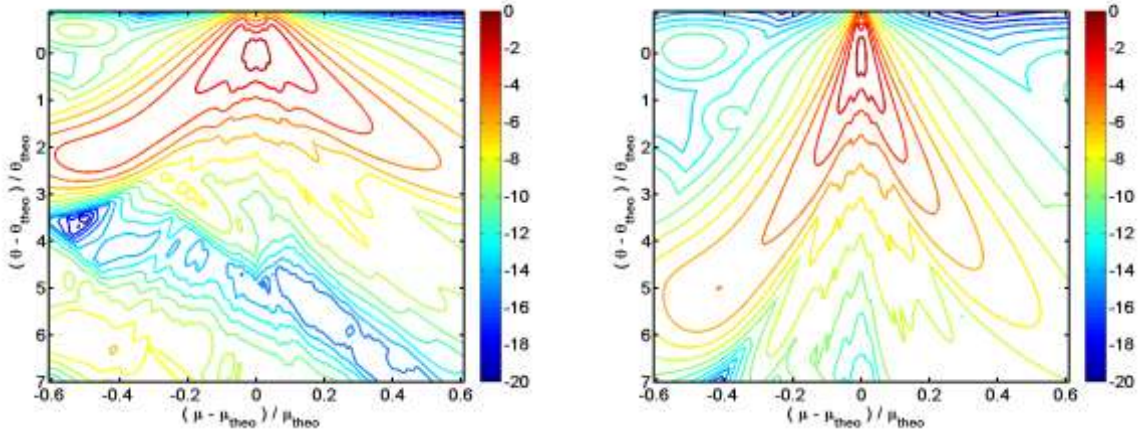

(a) (b)

Figure 6 - Contour plot of $\Delta(\mu, \theta)$ as function of the normalized Doppler rate error and of the normalized main lobe width error (a) for a perpendicular and non-midpoint crossing baseline, Case C and (b) for a smaller target size, Case D.

Figure 5 and Figure 6 show the contour plots related to $\Delta(\mu, \theta)$ (each normalized with respect to its maximum value) as a function of the normalized Doppler rate error and normalized main lobe width error. In all cases the highest value of $\Delta(\mu, \theta)$ occurs in (0,0): hence we can state that in all the cases studies both the Doppler rate and the main lobe width are well estimated; in accordance with eq. (4), assuming φ and y_0, known the complete kinematic parameters can be evaluated. The $\Delta(\mu, \theta)$ cut along Doppler rate axis and along the main lobe width axis are shown in Figure 7. As expected a peak in zero that corresponds to the Doppler rate and main lobe width of the target of interest is noted and also it is shown that a narrow peak is obtained for a smaller target (magenta line). This can be easily explained by investigating the target signature; smaller target has a large main lobe with more Doppler variation. We also note that the effect of pattern error is far less than that of Doppler rate error.

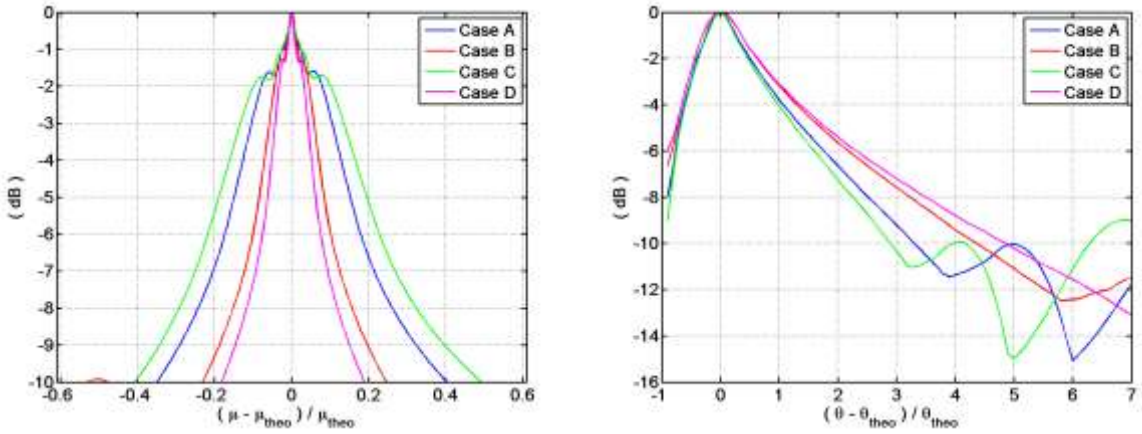

(a) (b)

Figure 7 - (a) $\Delta(\mu,\theta)$ cut along Doppler rate axis and (b) $\Delta(\mu,\theta)$ cut along the main lobe width axis

5. Application to real data

A passive FSR system was set-up to test the performance of the previously introduced approach where FM signals were exploited as signals of opportunity.

5.1 Acquisition campaign

The experimental campaign was carried out near "Leonardo Da Vinci" airport (Rome, Italy), looking at planes landing at the airport following the 16L runway. The distance L between the receiver Rx (located at seaside) and the transmitter Tx (Monte Gennaro), is about 56 km. In addition, it is also possible to retrieve the value of baseline crossing angle and baseline crossing point since the nominal altitude of the aircraft during its approach to the runway is known. At a first approximation, after projecting the positions of Tx, Rx and aircraft (when approaching the 16L runway) onto a 2D coordinate system by dropping the altitude information, the baseline crossing angle and the baseline crossing point are $\varphi = 10°$ and $y_0 = 4.961$ km, respectively. The multi-channel receiver is based on a direct Radio Frequency (RF) sampling approach. Proper band-pass filters, variable attenuators and amplifiers are used in the analogue section to reject out-of-band interferences and to match the A/D signal dynamic range. After digital down-conversion of the acquired signals, single FM channels of interest are extracted and stored for off-line processing, with a final sampling frequency F_s=200KHz. Specifically, FM channel 107.4 MHz ($\lambda \approx 2.8$m) is considered in the following sub-section. Directive FM antenna with a beamwidth of about 90° was used, pointed towards the selected transmitter.
A commercial ADS-B receiver was also employed in order to collect live navigation data for aircrafts landing at Fiumicino airport, to be used as ground-truth for velocity estimation.

5.2 Experimental results

Following the processing scheme introduced in Section 3, after the square law detector a decimation is performed by a factor 8^3, so that the acquired signal is down-sampled to F_{s2}=390.625 Hz, suitable for the not ambiguous observation of the target Doppler signature. In Figure 8(a) is reported the time domain signature of the received signal after the square law detector of an Airbus A319 with a horizontal and vertical dimension equal to 33.84 m and 11.76 m, respectively.

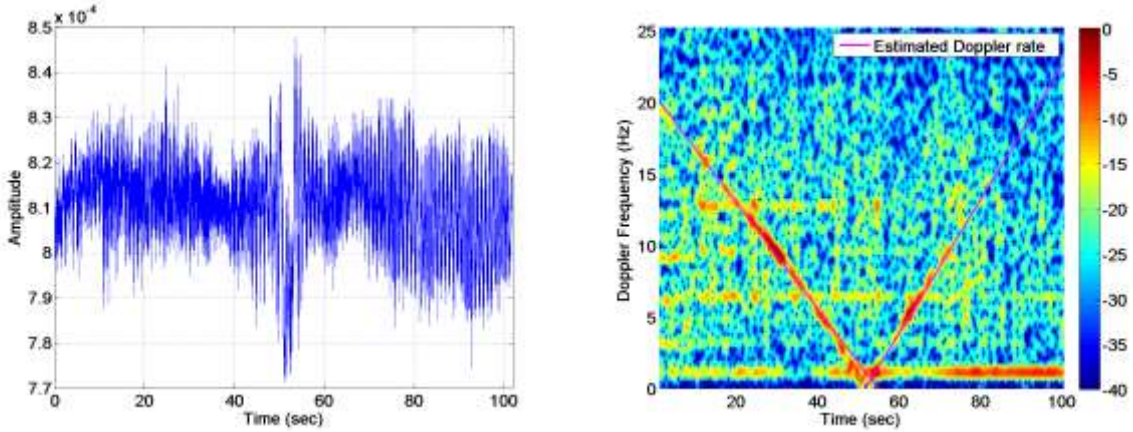

(a) (b)

Figure 8 - (a) Received signal after square law detector signature and (b) spectrogram.

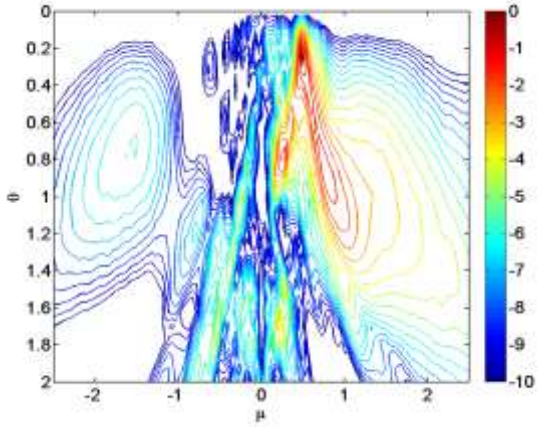

Figure 9 - Contour plot of $\Delta(\mu,\theta)$ as function of the Doppler rate and of the main lobe width.

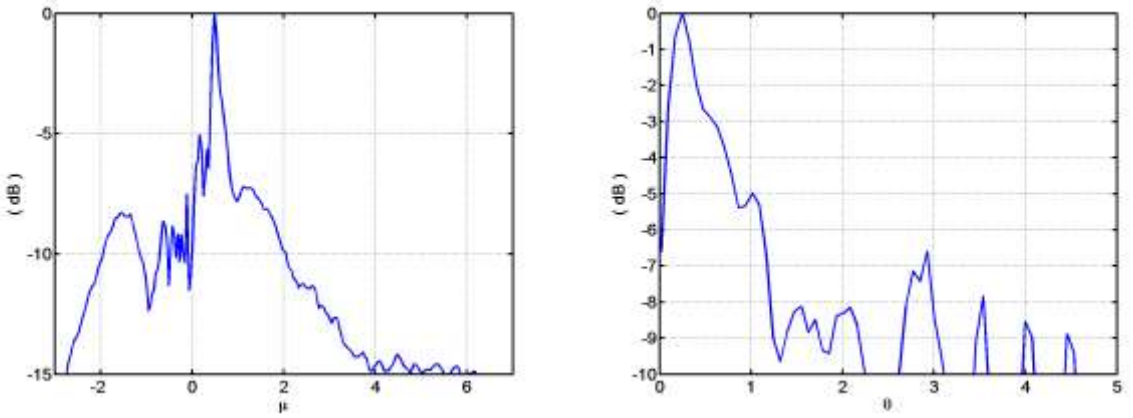

(a) (b)

Figure 10 - (a) $\Delta(\mu,\theta)$ cut along Doppler rate axis and (b) $\Delta(\mu,\theta)$ cut along the mainlobe width axis.

As it can be observed, the amplitude modulation due to the target movement is noticeable. Figure 8(b) shows the respective spectrogram (normalized with respect to its maximum value). A Hamming window for the estimation of the STFT is set equal to 2.56 sec. It is clear the correspondence between the spectrogram and the corresponding time Doppler signature in terms of crossing point located at 52 sec. As the target in this case do not cross the baseline in the middle and perpendicularly, the two branches of the spectrogram are not completely symmetrical. The Radon transform is performed to the spectrogram and two different Doppler rates are well estimated as shown in the Figure 8(b) with value equal to $\hat{\mu} = 0.4666$ and $\hat{\mu} =$

-0.3731. Then, the 2D filter bank is performed with the impulse response (eq. (7)) constructed considering different values of the Doppler rate in the range $\mu = [-6: 0.04: 6] + \hat{\mu}$ and different values of the main lobe width in the range $\theta = [0.1: 0.1: 8]\hat{\mu}\eta$. Figure 9 shows the contour plots related to $\Delta(\mu, \theta)$ (normalized with respect to its maximum value) as a function of the Doppler rate and of the main lobe width and it is clear the presence of a peak in correspondence of ($\tilde{\mu} = 0.4872, \tilde{\theta} = 0.2485$) as it is also shown in Figure 10. In accordance with the geometry introduced in Section 5.1, as the baseline crossing angle and the baseline crossing point are known it is possible to estimate the velocity in agreement with eq. (4), $\tilde{v} = 79.62$ m/s against $v = 72.07\ m/s$ provided by the ADS-B with 10.5% relative error.

6. Conclusion

In this paper we have presented a two-dimensional filter bank to address the issue of the unknown target dimensions and trajectory parameters to define the impulse response of the matched filter. The proposed approach is suitable for the velocity estimation of moving target in FSR geometry under the assumption that the baseline crossing point and baseline crossing angle are known. Simulated results in different case studies have been provided to show the correctness. Also, results achieved against FM based passive FSR data has been provided showing results in good accordance with the simulated data and showing the effectiveness of the proposed procedure.

References

[1] M. Gashinova, L. Daniel, V. Sizov, E. Hoare and M. Cherniakov, "Phenomenology of Doppler forward scatter radar for surface targets observation," in Radar, Sonar & Navigation, IET , vol.7, no.4, pp.422-432, April 2013.

[2] C. Hu, V. Sizov, M. Antoniou, M. Gashinova and M. Cherniakov, "Optimal Signal Processing in Ground-Based Forward Scatter Micro Radars," in *IEEE Transactions on Aerospace and Electronic Systems*, vol. 48, no. 4, pp. 3006-3026, October 2012.

[3] I. Suberviola, I. Mayordomo and J. Mendizabal, "Experimental Results of Air Target Detection With a GPS Forward-Scattering Radar," in IEEE Geoscience and Remote Sensing Letters, vol. 9, no. 1, pp. 47-51, Jan. 2012.

[4] D. Pastina, M. Contu, P. Lombardo, M. Gashinova, A. De Luca, L. Daniel and M. Cherniakov, "Target motion estimation via multi-node forward scatter radar system," in IET Radar, Sonar & Navigation, vol. 10, no. 1, pp. 3-14, 1 2016.

[5] A. De Luca, M. Contu, S. Hristov, L. Daniel, M. Gashinova and M. Cherniakov, "FSR velocity estimation using spectrogram," 2016 17th International Radar Symposium (IRS), Krakow, 2016, pp. 1-5.

[6] M. Contu, A. De Luca, S. Hristov, L. Daniel, A. Stove, M. Gashinova, M. Cherniakov , D. Pastina, P. Lombardo, A. Baruzzi, D. Cristallini "Passive Multi-frequency Forward-Scatter Radar Measurements of Airborne Targets using Broadcasting Signals", IEEE Transactions on Aerospace and Electronic Systems, in print.

[7] N.Ustalli, D.Pastina and P.Lombardo, "Theoretical performance prediction for the detection of moving targets with Forward Scatter Radar Systems", 2016 17th International Radar Symposium (IRS), Krakow, 2016, pp.1-6.

[8] Oppenheim, Alan V., Ronald W. Schafer, and John R. Buck. Discrete-Time Signal Processing. 2nd Ed. Upper Saddle River, NJ: Prentice Hall, 1999.

[9] Lim, Jae S., Two-Dimensional Signal and Image Processing, Englewood Cliffs, NJ, Prentice Hall.